Transportation Research Part A 208 (2026) 104986

Contents lists available at ScienceDirect

Transportation Research Part A

journal homepage: www.elsevier.com/locate/tra

A capacity framework for pedestrian infrastructures under physical distancing regulations: A guide for crowd monitoring and management

Lucia van Schaik, Dorine Duives *, Serge Hoogendoorn

Department of Transport & Planning, Delft University of Technology, Stevinweg 1, PO Box 5048, 2600 GA Delft, the Netherlands

ARTICLE INFO

Keywords:
Capacity framework
Physical distancing
Respiratory virus
SARS-CoV-2
COVID-19 pandemic
Pedestrian operational movement dynamics
Crowd monitoring
Crowd management

ABSTRACT

At the end of 2019, SARS-CoV-2 rapidly spread across the globe within a few months. Since then, tackling the virus has been high on national agendas for over three years. As with other respiratory viruses, physical distancing (i.e., requiring sufficient space between individuals) became a key measure to prevent airborne virus transmission between individuals. However, this measure significantly reduces the capacity of pedestrian infrastructure, as more space is needed between people. This paper develops a capacity framework designed to calculate the capacity of pedestrian infrastructure, evaluate its state, and propose tailored interventions when physical distancing regulations are enforced. The framework is founded on the current state-of-the-art in pedestrian operational movement dynamics and determines capacity using three independent key performance indicators: flow rate, density, and interactions. Through two case studies from the COVID-19 pandemic, this paper demonstrates how the framework identifies when and why pedestrian infrastructures become unsafe and enables targeted interventions. The framework's relevance extends beyond the COVID-19 pandemic, offering insights into crowd management and resilient pedestrian infrastructure design for future airborne disease outbreaks.

1. Introduction

Originating in Wuhan, China, in December 2019, SARS-CoV-2 spread rapidly worldwide, causing the COVID-19 pandemic (COVID-19 is the disease caused by the virus). Since then, at least 760 million cases and 6.9 million deaths have been reported worldwide (World Health Organization, 2024). The World Health Organization classified the pandemic as a public health emergency of international concern (PHEIC) from January 30, 2020, to May 5, 2023 (Reuters, 2024).

Like other respiratory viruses, SARS-CoV-2 predominantly transfers between individuals through droplet spread, aerosol spread, and fomite transmission (Atamer Balkan et al., 2024). To limit the propagation of the virus throughout the world and countries, drastic but diverse measures have been taken at the national level. Traffic of goods and people through Europe has been limited for months, restaurants and hotels have been closed in many countries, and most people have been asked to work from home. Most importantly, physical distancing has been issued in most EU countries pertaining to interactions with unrelated individuals to enable people to perform most daily activities again. Physical distancing, a non-pharmaceutical intervention, incites people to keep their physical distance from other unrelated individuals and refrain from social interactions such as shaking hands, hugging, and embracing. The

* Corresponding author.
E-mail addresses: l.vanschaik@tudelft.nl (L. van Schaik), d.c.duives@tudelft.nl (D. Duives), s.p.hoogendoorn@tudelft.nl (S. Hoogendoorn).

https://doi.org/10.1016/j.tra.2026.104986
Received 14 August 2020; Received in revised form 1 December 2024; Accepted 17 March 2026
Available online 26 March 2026

exact details of physical distancing regulations vary by country, from 1.0 m recommended by the World Health Organization (2020) to 6 feet (1.82 m) cited by the U.S. Centers for Disease Control and Prevention (2020).

As a result of the physical distancing regulations, the capacity of pedestrian infrastructure across the globe has plummeted. For example, the capacity of the main shopping street in Amsterdam, named de Kalverstraat, can only host 12% (3736P/h) of its original capacity (30.857P/h) (Duives et al., 2020). While parks, shopping areas, and transfer hubs could easily cope with demand before the COVID-19 outbreak, most pedestrian infrastructure is now running at capacity. City officials struggled with two questions, namely 1. 'What characteristics of the space and crowd dynamics determine the new COVID-19"safe" capacity of pedestrian infrastructure?' and 2. 'What methodology can be used to evaluate whether a pedestrian infrastructure currently exceeds the COVID-19"safe" capacity?'. Here, capacity is defined as the total number of people that can reside in a particular area at the same time performing a variety of actions (e.g., walking, standing still, queueing), and the 'safe' capacity refers to the capacity at which the chance of contagion is minimized according to the latest guidelines of a particular country.

This paper aims to develop a capacity framework that can be used to determine the capacity of pedestrian infrastructure, evaluate its state, and propose tailored interventions when physical distancing regulations are in place. The current state-of-the-art in pedestrian operational movement dynamics will serve as a basis for this framework and the underlying key performance indicators (KPIs). Please note that this paper will not discuss the epidemiological reasoning on which the physical distancing regulations are founded but will adopt these as the starting point for the development of the capacity framework. Given that little is known about pedestrian operational movement dynamics during the physical distancing era to build on, logical reasoning is used to specify the framework and KPIs further. Afterward, the physical distancing capacity framework is applied to two practical case studies during the COVID-19 pandemic to demonstrate its usage. Additionally, we will reflect on the usability of the new framework in supporting real-time management, evaluation, and design of pedestrian infrastructure during a respiratory virus pandemic.

This paper contributes to the state-of-the-art in two ways. First, the paper provides an overview of lessons the authors learned during the rapid prototyping of this capacity framework during the COVID-19 pandemic. Second, and more importantly, the framework offers a tool to quickly develop real-time crowd monitoring and management schemes for pedestrian infrastructure during future respiratory virus pandemics. In addition, the framework allows us to evaluate to what extent the pedestrian infrastructure is prepared for a new pandemic featuring an airborne disease.

This paper will continue as follows. First, section 2 discusses the state-of-the-art capacity frameworks for pedestrian infrastructures and the physical distancing regulations during the COVID-19 pandemic in several countries, including the Netherlands. Section 3 details the new physical distancing capacity framework and underlying KPIs accordingly. Sections 4 and 5 introduce the two case studies and demonstrate the application of the physical distancing capacity framework in these two cases. Section 6 discusses the lessons derived from these two case studies. Section 7 discusses the applicability of the new framework for the design and management of pedestrian infrastructure during a respiratory virus pandemic in the future. The last section concludes this paper with a brief discussion and some indications of future work.

2. State-of-the-art on pedestrian capacity frameworks and physical distancing regulations

To develop a physical distancing capacity framework, first, a good insight into the literature pertaining to existing capacity frameworks is required. Besides that, it is essential to understand the requirements of the new framework. In this case, the requirements predominantly feature the physical distancing regulations in various countries during the COVID-19 pandemic. The discussion will first cover existing capacity frameworks, followed by an overview of the physical distancing regulations of various countries during the COVID-19 pandemic.

2.1. Developments in pedestrian capacity frameworks

Greenshields et al. (1935) presented a parameterization of traffic behavior. They introduced the relation of traffic flow ($q = k \cdot u$) and found that there is a limit to the number of vehicles that can move through a particular cross-section. This natural limit on the flow rate is coined flow rate capacity. Besides that, Greenshields et al. (1935) also showed a natural limit to the number of vehicles one can statically store on a road stretch, often called the jam density or storage capacity.

Until 1971, only a fundamental relation featuring vehicular traffic on a one-dimensional stretch of road existed. At that time, Fruin (1971b) introduced a parameterization of this fundamental relation for pedestrians, which relates the flow rate to a two-dimensional area instead of a one-dimensional line. Besides that, he presented a Pedestrian Level-of-Service (PLoS) concept, which translated the quantitative description of the crowd movements into a qualitative assessment of the crowdedness (Fruin, 1971a). Even though very progressive, a general disadvantage of Fruin's PLoS framework is that it does not consider the temporal dimension and contextual dynamics of pedestrian traffic.

In the years to follow, several studies attempted to incorporate the situational context into the seminal work of Fruin (e.g., Landis et al. (2001); Bian et al. (2007)). In 2008, Dowling et al. (2008) reviewed the PLoS models developed up to that year and established that the variables of most adaptations of Fruin's PLoS model are not generalizable and depend heavily on the context for which the PLoS model was initially estimated. More recent reviews by Raad et al. (2017) and Banerjee et al. (2018) show that this has changed since 2008. That is, the macroscopic flow variables density and flow are still at the basis of most PLoS frameworks. More recent PLoS models mainly added geometric infrastructure characteristics (e.g., walkway width, gradient, and crosswalk distance), traffic characteristics (e.g., roadway volume, pedestrian speed, and delay time), or user characteristics (e.g., age, gender, and noncompliance rate) to the model formulation. Recently, researchers started studying the impact of time and perception on PLoS (e.g., van Gelder (2018);

Finch (2010); Grolle (2016); Raad and Burke, (2017) and Hoskam (2017)). Compared to Fruin's PLoS model, most recent PLoS frameworks are better equipped to handle the complexity of urban traffic. However, under these exceptional circumstances of physical distancing regulations, none of the PLoS frameworks applies because we assume that the pedestrian operational movement dynamics changed on which the framework was founded.

Another way to identify the capacity of pedestrian infrastructure is by directly using the pedestrian fundamental diagram (P-FD). Since 1971, many scientists have further detailed the fundamental relation for pedestrian traffic and added additional levels of complexity. Most researchers studied the impact of various movement base cases on the P-FD and capacity (e.g., Seyfried et al. (2007); Kretz et al. (2006); Zhang et al. (2011) and Cao et al. (2017)). Other researchers explored the impact of the context and population on the P-FD and capacity (e.g., Daamen and Hoogendoorn (2010); Garcimartin et al. (2014); Subaih et al., 2019; Haghani et al. (2020)). A last group of studies included the impact of various cultures on the P-FD (e.g., Chattaraja et al. (2009)). The main benefit of the P-FD is that it is a quantitative relation, which allows crowd managers to objectify their decision-making.

However, the question is whether the P-FD is applicable during a respiratory virus pandemic. Firstly, because we assume that not all pedestrians will adhere to the physical distancing regulations. Initially, the P-FD was limited by means of a natural limit. People are physically unable to move faster because the presence of others constricts their movements. This natural limit is far less stringent when the physical distancing regulations apply because of the large difference between the minimal required physical distance to protect the crowds' health and the minimum required physical distance to be able to move.

Constricted movements will still arise if all people strictly follow the regulations. Yet, we expect the behavior of pedestrians near capacity to change due to the lack of physical constriction. In contrast to 'normal' capacity restrictions, people can still walk freely and are thus expected to retain a relatively higher speed when the physical distancing capacity of a pedestrian infrastructure is almost reached. Thus, we expect that the part of the speed-density relation leading up to the capacity has a different shape under physical distancing circumstances.

Given the large role of rule compliance and the potential changes in walking dynamics, using a contextual fitting P-FD to determine the limit of a pedestrian infrastructure will not suffice. Instead, a framework is needed that computes the 'safe' capacity for pandemics such as the COVID-19 pandemic based on the latest epidemiological insights regarding the necessary physical distance to curb respiratory virus transmission and the crowd's capabilities to retain their distance in a theoretically safe infrastructure.

2.2. Physical distancing regulations across countries

During the COVID-19 pandemic, various governing bodies, universities, and health agencies drafted physical distancing regulations to limit virus transmission between non-household members. This refers to the minimal acceptable distance from body surface to body surface between unrelated individuals. For example, two students living together are considered related, but a father and son in separate households are not.

A quick search on the internet reveals that various countries apply different distances for the physical distancing regulations. The World Health Organization (2020) and France (Gouvernement.fr, 2020) specify the lowest physical distance that should be adhered to between unrelated individuals, which is 1.0 m. The maximum physical distance is instigated by, amongst others, the United Kingdom (BBC.com, 2020), namely 2.0 m. Many countries have physical distancing regulations in the middle of this spectrum. Germany, Spain, and the Netherlands stipulated a physical distance of 1.50 m (Spain.info, 2020; Bundesregierung.de, 2020; Rijksinstituut voor Volksgezondheid en Milieu, 2020). In the United States, the Centers for Disease Control and Prevention (2020) specifies 6 feet (1.82 m). Given the variation between countries, a physical distancing capacity framework must be flexible enough to cope with these varying physical distancing regulations.

Besides, most countries stipulate additional safety precautions and allow infringements on the physical distancing regulations when keeping the required distance between unrelated individuals is challenging. For example, in France and Spain, facial masks are required in a large number of crowded tourist areas, and in most EU countries, facial masks are made obligatory in public transit (Spain.info, 2020; Gouvernement.fr, 2020). In addition, educational facilities for children and teens, such as primary and secondary schools, feature less stringent regulations in many countries, including the Netherlands (Rijksinstituut voor Volksgezondheid en Milieu, 2020). Yet, most governing bodies are adamant that physical distancing is preferred over close contact between individuals wearing a facial mask in those cases (e.g., Rijksinstituut voor Volksgezondheid en Milieu, 2020). Thus, even though the physical distancing capacity framework should be able to cope with local variations in the physical distancing regulations, it remains essential to, also in those situations, still attempt to enforce the country-specific general physical distancing regulations.

3. Designing the physical distancing capacity framework

This section outlines the key design choices made in developing the new physical distancing capacity framework. First, the framework's program of requirements is described. Next, the design strategy is explained, and an overview of the framework's general structure is provided. Then, the minimum space requirements for pedestrians are presented and parameterized. Finally, the subsequent three sections delve into the framework's three key performance indicators (KPIs): flow rate, density, and interactions.

3.1. Requirements for the physical distancing capacity framework

The authors have been involved in discussions with various Dutch municipalities pertaining to the capacity of crowded pedestrian infrastructure during the COVID-19 pandemic. Based on these discussions, five general requirements for the new framework were

identified.

Requirement 1. Rules and regulations – The framework should be flexible concerning the local physical distancing regulations. As mentioned before, the physical distancing regulations vary heavily between countries. Moreover, differences in COVID-19 rules and regulations between functionally distinct pedestrian infrastructures (e.g., public transit, education, and touristic areas) are observed (Rijksinstituut voor Volksgezondheid en Milieu, 2024). Thus, the framework should be flexible in terms of local physical distancing regulations.

Requirement 2. Spatial layout – The framework should be flexible concerning the spatial layout of the pedestrian infrastructure. Pedestrian infrastructure is very diverse. It ranges from general-purpose traffic streets with a pedestrian path to crowded squares. It is important that the new physical distancing capacity framework can be used to monitor a wide variety of pedestrian infrastructure. This requires the framework to be flexible concerning the spatial dimensions of the infrastructure. In particular, the width of the total walkable area should be an input of the framework and how to deal with obstacles in this walkable area.

Requirement 3. Functional layout – The framework should be flexible concerning the functional layout of the infrastructure. Infrastructure can have different functions, including walking, waiting, and queueing. It is imperative that the framework can signal capacity breaches for all these functionally different infrastructures. Depending on the function of the infrastructure, potentially different traffic flow variables should be used to monitor this infrastructure. Thus, the physical distancing capacity framework should either incorporate the function of the infrastructure as an input or be able to, irrespective of the function, signal when the physical distancing regulations are violated.

Requirement 4. Compliance dependent – The framework should be able to identify compliance behavior with the physical distancing regulations. The framework assumes pedestrians attempt to follow the rules and regulations. However, our experiences during the COVID-19 pandemic show that this intention does not always lead to rule compliance (van Schaik et al., 2024). Accidentally or purposefully, pedestrians violate the physical distancing regulations, even when there are few other pedestrians around. A physical distancing capacity framework must signal issues resulting from non-compliance. For instance, it should signal when people are standing too close to each other while the theoretical limits of the pedestrian infrastructure have not yet been met.

Requirement 5. Real-time evaluation – It is challenging to predict how many pedestrians will reside in a particular area at a given moment. Thus, most municipalities want to use the physical distancing capacity framework to monitor and evaluate pedestrian infrastructure in real-time. This requirement means only variables can be used in the framework that one can monitor and compute in real-time. For most crowd monitoring systems, this is a very limited set of variables featuring, amongst other things, flow rate, density, and the location of all pedestrians in the field of view.

3.2. Design strategy and layout of the physical distancing capacity framework

The five requirements detailed in the previous section are used as the foundation of the new physical distancing capacity framework. The relations between the requirements identified in section 3.1 and the elements of the framework presented below are shown in Fig. 2 at the end of this section.

To this end, we propose a 'scenario-based' method, where the scenarios refer to situations that are (potentially) unsafe in terms of airborne virus transmission. In doing so, we make the framework generic, where the scenarios cater to the specific characteristics of the infrastructure considered.

In this study, three specific scenarios are considered in which potential airborne virus transmission pathways are triggered:

1. Too many people attempt to move through a limited cross-section,
2. Too many people are standing, queueing, or waiting in a limited space, and
3. People do not comply with physical distancing regulations even though there is enough space.

These scenarios are based on current knowledge of the SARS-CoV-2 transmission pathways. More scenarios can be included in this list when scientists identify new pathways.

The difference between scenarios 1 and 2 pertains to the operational movement dynamics of the pedestrians (i.e., in scenario 1, they are moving, while in scenario 2, they are stationary). In an unidirectional homogeneously distributed crowd, scenarios 1 and 2 are equivalent. However, even in unidirectional streets, pedestrians tend to overtake one another due to speed heterogeneity. As a result, the theoretical maximum density of a crowd walking through a street is often smaller than the theoretical maximum density of a stationary crowd in that same street. The difference between scenarios 1 and 2 compared to scenario 3 pertains to the compliance of the pedestrians with the regulations. As such, this last scenario is related to the behavioral maximum capacity of a space.

These three scenarios can be monitored using three different traffic flow variables. The first scenario is related to the number of pedestrians walking through a street for a short period, which can be monitored using the flow rate. The second scenario concerns the maximum number of people that can stand still in a pedestrian area, which can be monitored using the density. The third scenario is related to the distance between individuals, which can be monitored via the headway. In particular, headways smaller than the physical distancing regulation between pedestrians are of interest in relation to airborne virus transmission. Instead of incorporating the headway directly, we have transformed the headways into the number of interactions with a headway smaller than 1.50 m (the physical distancing regulation stipulated by the Dutch government). Hereafter, we coin this third variable 'interactions KPI' in the remainder of this paper. Only the latest crowd monitoring systems allow for the computation of this variable. For each variable, from here on called KPI, the current value of the KPI is compared to the KPI threshold to derive the state of the pedestrian infrastructure $S_{KPI}(t)$ utilizing Eqs. (1)–(4). Here, $q(t)$, $k(t)$, and $I(t)$ represent the measured flow rate, density, and interactions recorded by the

monitoring system. $S_q(t)$, $S_k(t)$, and $S_I(t)$ are the normalized flow rate, density, and interactions KPIs at time t. The state is normalized by means of the three thresholds (i.e., T_q, T_k, and T_I). The exact definition of all three KPIs and their thresholds are described in the following section.

$$S_q(t) = \frac{q(t)}{T_q} \tag{1}$$

$$S_k(t) = \frac{k(t)}{T_k} \tag{2}$$

$$S_I(t) = \frac{I(t)}{T_I} \tag{3}$$

$$S_{KPI}(t) = \min\left(1, \max\left(S_q(t), S_k(t), S_I(t)\right)\right) \tag{4}$$

In general, we would expect scenario 3 to be the first scenario to occur because it requires the lowest number of pedestrians to be activated. Yet, theoretically, both scenarios 1 and 3 can arise without the others being triggered beforehand. Consequently, to monitor the physical distancing capacity of pedestrian infrastructure, we need to monitor all three KPIs simultaneously. This means that our framework comprises three KPIs, which jointly provide insight into the status of the pedestrian infrastructure. The framework is visualized in Fig. 1. Here, the state of the metric that is relatively closest to its threshold (i.e., the red dial) determines the state of the pedestrian infrastructure $S_{KPI}(t)$. The maximum value of the dial is capped at 1 (see Eq. (4)) to allow for a precise interpretation and visualization of the physical distancing capacity state.

Please note that the threshold on each KPI varies over space because it depends on the local context (i.e., spatial layout). Moreover, the thresholds also vary over time at a given location because the thresholds are dependent on group dynamics and the function(s) of the pedestrian infrastructure. The function of pedestrian infrastructure, for example, market squares or general-purpose streets, also affects the walkable area and, as such, the maximum acceptable flow rate. The presence of groups of related individuals in a crowd increases the thresholds on all three KPIs, where the extent to which the threshold varies depends on the distribution of group sizes, the spatial formation of the individual groups, and the spatial distribution of groups over the crowd.

In this paper, we will detail how to incorporate the function of pedestrian infrastructure and provide some first suggestions regarding the implementation of group dynamics in the framework. However, to limit the complexity of the paper, we will refrain from comprehensively describing how to deal with group dynamics in the physical distancing capacity framework. More elaborate research is required to fully incorporate group dynamics into the framework.

Fig. 2 shows the relation between the five requirements presented in section 3.1 and the framework's elements. In essence, the framework consists of a set of metrics that can be adapted for each new context and use case. The need for real-time evaluation, crowd compliance, the functional layout, and the spatial layout pose requirements on the type of metrics. Each metric M_n features a state $S_n(t)$ and a threshold T_n. The state is determined by the layout, the function of the infrastructure, and the crowd's compliance. The thresholds of each state are partly determined by the governing rules and regulations, as well as the functional layout of the infrastructure.

3.3. Minimum space requirements for pedestrians during COVID-19

We determine the KPI thresholds for the Dutch situation, where the minimum physical distance of 1.50 m is adopted. Given this physical distancing regulation and the average circumference of a pedestrian of 0.45 m x 0.60 m (length x width) Fruin (1971a, b), the minimum space requirement of one single pedestrian is 1.95 m x 2.10 m (length x width). The reader is referred to Fig. 3 for a parameterization of the minimum space requirement, where the body width d_{lat} is 0.60 m, the body length d_{lon} is 0.45 m, and the required physical distance d_{PD} is set to 1.50 m (i.e., 0.75 m on each side).

If two individuals belong to one household and walk together as a group, the space requirements between them diminish. Studies featuring the spatial layout of two-person groups identify that these groups mainly walk abreast. As such, the lateral space requirement of a group increases concerning the lateral space requirement of a single pedestrian. We assume a distance between two individuals of

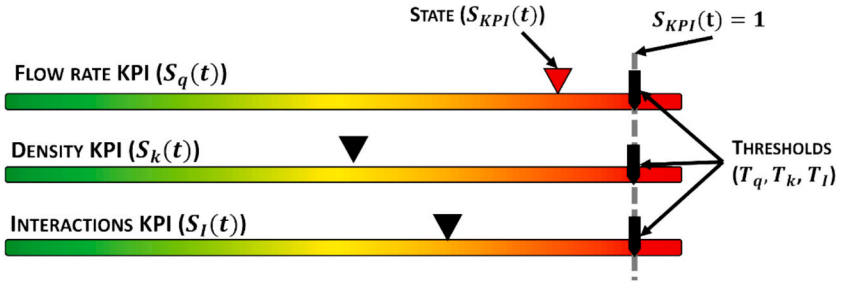

Fig. 1. Visual impression of the physical distancing capacity framework.

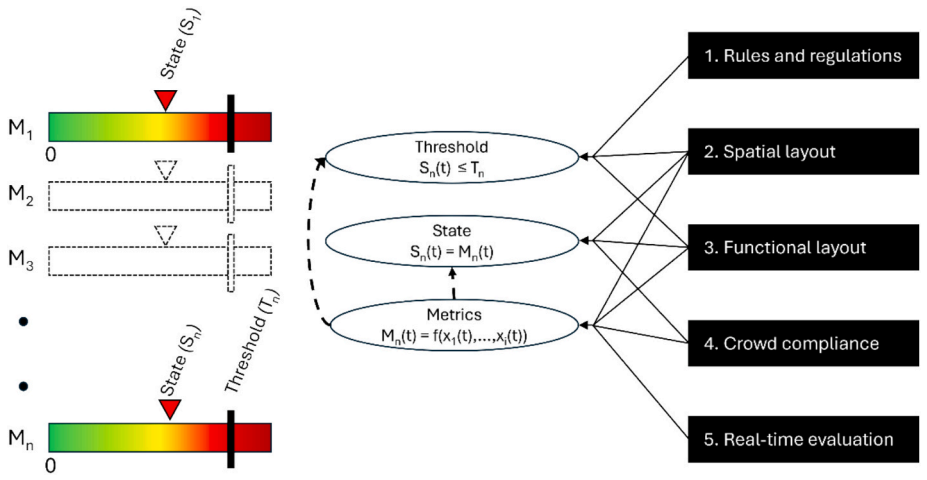

Fig. 2. Relation between the physical distancing capacity framework and the functional requirements.

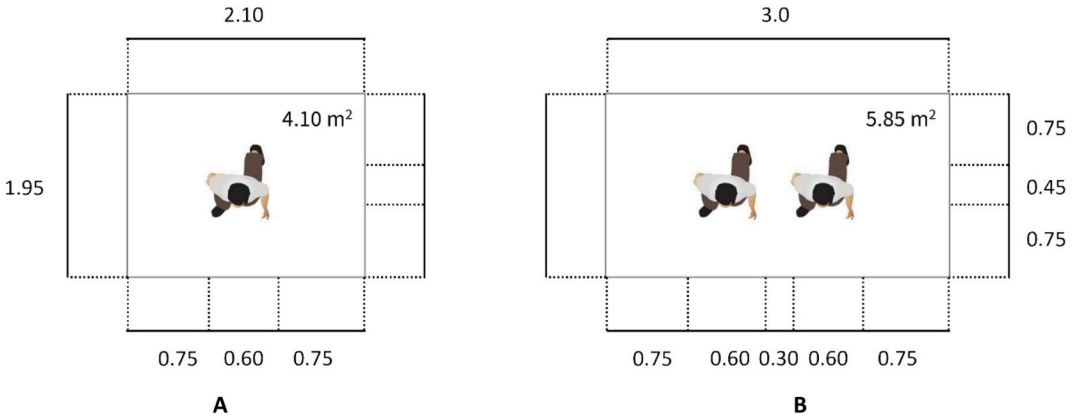

Fig. 3. Specification of the minimum space requirements for single pedestrians (A) and pairs (B).

the same group d_{group} of 0.30 m, which results in an interpersonal distance of 0.90 m between the center points of mass of two individuals. This interpersonal distance is slightly larger than the interpersonal distance identified by Moussaïd et al. (2010); Zanlungo et al. (2014), and Gorrini et al. (2015) of roughly 0.78 m for situations with relatively high densities. We assumed a slightly larger interpersonal distance because we expect that group members experience less pressure to stay closely together during low densities. As a result, the total lateral space requirement of a 2-person group (pair) is 3.0 m. A pair's longitudinal space requirement remains 1.95 m.

For three or more individuals walking together, the computation of the minimum space requirement per group becomes more complex because the spatial layout of three persons can vary (Zanlungo et al., 2015). These groups can take up a lot of lateral space when walking abreast or have an increased lateral and longitudinal space requirement when walking in a back- or forward-pointing V-shape. In such cases, the maximum lateral and longitudinal dimensions of the convex hull of the outwards pointing boundaries of each group member determine the minimum space requirement. In the case of three and four-person groups, the minimum convex hull is achieved when three individuals walk abreast or when two groups of two people walk behind each other.

3.4. Flow rate computation and threshold determination

The flow rate $q(t)$ is defined as the number of pedestrians that walk across a specific cross-section during a predefined period. Using smart counting sensors (i.e., HD camera + computer vision algorithms, stereovision cameras, or depth sensors), moving objects in pedestrian infrastructure can be detected precisely. These object traces (id number, x, y, t) are translated in counts, a.k.a. the number of traces found on both sides of a cross-section within a predefined period (see Eq. (5)). Here, N_{in} and N_{out} refer to the number of people moving in two directions across a cross-section in period Δt.

$$q(t) = \frac{N_{in} + N_{out}}{\Delta t} \tag{5}$$

For monitoring purposes, these counts are often aggregated per minute (Daamen et al., 2016). Yet, recent experiences have shown that pedestrian flows in pedestrian infrastructure tend to be very unstable (see the two cases in this paper). Consequently, a shorter aggregation period is required to capture the short bursts in which too many people congregate in space. Thus, a period of 15 s is adopted. This period is long enough to capture the peaks in the flow rate and short enough to prevent over-conservative assessment by the physical distancing capacity framework.

The physical distancing capacity framework is mainly used for general-purpose scenarios in pedestrian infrastructure. Here, we assume that the general scenario the framework should be able to cope with is a bidirectional traffic scenario featuring a crowd with a heterogeneous speed distribution. To allow for overtaking and bidirectional traffic, the flow rate threshold is limited by the number of discrete lanes (i.e., one-directional moving queues) that simultaneously fit within the minimum cross-section of a corridor. A more efficient stacking of pedestrians in space (i.e., in a hexagon shape) would automatically violate the physical distancing regulations when pedestrians attempt to overtake or move across the same cross-section in opposite directions.

The flow rate threshold T_q depends on the spatial layout and the local pedestrian operational movement dynamics. In the longitudinal direction, the flow rate threshold is limited by the average walking speed of the crowd and the minimum distance headway that individuals have to adhere to. Here, the longitudinal spacing is equal to the physical distancing rules of the respective country where the framework is adopted (i.e., 1.50 m in the Dutch case).

Given the fundamental relation between flow rate, headway, and speed, one can translate these details into the flow rate threshold T_q using Eqs. (6)–(8).

$$L = \begin{cases} 1 & w < 2d_{shy} + 2d_{lat} + d_{PD} \\ 2 + \left\lfloor \dfrac{w - 2d_{shy} + 2d_{lat} + d_{PD}}{d_{PD} + d_{lat}} \right\rfloor & w \geq 2d_{shy} + 2d_{lat} + d_{PD} \end{cases} \tag{6}$$

$$q_{lane}{}^{max} = \frac{60}{\frac{(d_{lon} + d_{PD})}{\bar{v}}} \tag{7}$$

$$T_q = L \cdot q_{lane}^{max} \tag{8}$$

where L represents the number of lanes, w the width of the corridor, d_{shy} the shy away distance from the wall, d_{lat} the lateral width of an average pedestrian, d_{lon} the length of a pedestrian, d_{PD} the minimum physical distancing requirement, q_{lane}^{max} the total number of pedestrians per lane that can pass in one minute, and $\bar{v}$ the average speed of the crowd. Please note that the number of lanes is an integer. For the 'simple' scenario of a straight corridor without obstacles, Table 1 depicts an example computation of the flow rate threshold T_q.

When obstacles are present in the corridor (e.g., trees, dustbins, sensing equipment), the computation slightly changes, given that obstacles alter the layout of the walkable space. The obstacles can hinder the optimal distribution of pedestrians over space. To estimate the impact of the obstacles, the threshold should be computed twice, once using the original computation method and once while treating the available gaps along the cross-section as separate corridors. The normative flow rate threshold is the smaller of the two resulting capacities (see Table 2 for the example calculation for a road stretch with an unfortunate obstacle).

When groups are present at the location, the flow rate threshold computation becomes far more complex due to the rapidly growing combinatorial complexity of the distributions of groups of different sizes of time and space. In general, groups of pedestrians require

Table 1
Example computation of the flow rate threshold T_q without obstacles.

Infrastructure and population characteristics
Width of the corridor $w = 5.70$ m
Average walking speed $\bar{v} = 1.0$ m/s
Physical distancing requirement $d_{PD} = 1.50$ m
Shy away distance $d_{shy} = 0.20$ m
Width of an average person $d_{lat} = 0.60$ m
Length of an average person $d_{lon} = 0.45$ m
Computation maximum flow rate per lane
Total longitudinal spacing = 1.50 + 0.45 = 1.95 m
Time required for one person to pass the cross-section safely = 1.95 / 1.0 = 1.95 s
Total number of pedestrians per lane that can pass in one minute $q_{lane}^{max} = 60 / 1.95 = 30.77$ persons per lane
Computation number of lanes
The width of the corridor is larger than 3.10 m (i.e., 2 · 0.20 + 2 · 0.60 + 1.50), and
The required space per extra pedestrian is 2.10 m (i.e., 0.60 + 1.50), so:
Number of lanes $L = 2 + \text{floor}((5.70 - 3.10)/2.10) = 3$ lanes
Flow rate threshold
Flow rate threshold $T_q = 3 \cdot 30.77 = 92.31$ persons per minute = 1.54 persons per second

less space than single pedestrians. Thus, more pairs than singles can pass the same cross-section during the same period. Consequently, the flow rate threshold identified in this paper based on the crowd's movement featuring only single pedestrians is a conservative estimation of the 'safe' capacity.

Yet, due to the assumption of bidirectional traffic featuring a heterogeneous crowd, extending the lane concept is impossible. Another solution is to fall back to the fundamental relation $q = k \cdot u$, and determine the flow rate threshold using the average walking speed of the crowd $\bar{v}$, the density threshold T_k, and the minimum available width of the cross-section $w_{available}$ using Eq. (9). Here, T_k can be made dependent on the distribution of groups and group sizes over time, as shown in section 3.5. However, this second solution will most likely result in a threshold that is too loose. Both solutions will have unwanted side effects, i.e., ineffective use of the infrastructure or public health risks. As such, more research is required regarding a fitting solution to incorporate group dynamics into the flow rate KPI. In the meantime, the lane concept will be used in the remainder of this paper to determine the flow rate threshold.

$$\mathrm{T_q} = \mathrm{T_k} \cdot \bar{v} \cdot w_{available} \tag{9}$$

3.5. Density computation and threshold determination

Besides flow rate, the crowd's density $k(t)$ is adopted as one of the KPIs, where density is defined as the number of people that reside within a predefined space simultaneously. Besides information pertaining to the flow rate, most smart counting systems can provide information pertaining to the number of pedestrians in the field of view $N(t)$. When combining this data with knowledge of the size of the area A captured within the field of view, the density can be derived using Eq. (10).

$$k(t) = \frac{N(t)}{A} \tag{10}$$

Similarly to the flow rate, densities are often recorded once per minute. However, given the fast-changing dynamics of bidirectional crowd movements, this would limit our ability to spot dangerous situations with a limited temporal timespan. Thus, this framework also records the density at a relatively high frequency every 15 s.

Next, we determine the density threshold T_k. Lagrange showed that the maximum density of circles in an area is achieved using hexagonal packing (Chang and Wang, 2010). Also, a similar packing results in the highest possible physical distancing density in case of pedestrian crowds, provided that we assume pedestrians are round. Yet, to achieve this packing in a corridor without violating the physical distancing rules, the corridor can only be loaded and unloaded in one direction. All pedestrians should walk into the area from one side while equally distributed across the cross-section before coming to a standstill during the loading process. Similarly, all pedestrians should walk out of the area on the other side while equally distributed across the cross-section, where the front row starts walking first. However, we assumed bidirectional traffic in most pedestrian infrastructure. Thus, to allow for bidirectional traffic and overtaking, spaces' optimal safe storage capacity is achieved when each individual is surrounded by a square box with the dimensions mentioned in Fig. 3. When we assume an even distribution of pedestrians over an infinite space, this results in a density threshold of $T_k = \frac{1}{2.10 \cdot 1.95} = 0.244 P/m^2$ in any given area.

Please note that $0.244 \mathrm{P/m^2}$ is a very optimistic threshold, given that streets will generally not permit the rectangular squares to be stacked optimally. However, as most pedestrian infrastructure is not entirely straight, a computation in which the greatest integer number of people that would jointly fit in the minimum width and length of the vision field of the sensor would result in a conservative estimation. That is, too much available walking space might not be accounted for when using an area's minimum width and length. In this case, an optimistic density threshold is preferred over a threshold that is too conservative.

Table 2
Example computation of the flow rate threshold $\mathrm{T_q}$ with an obstacle.

Additional infrastructure characteristics
Location of the obstacle (e.g., a tree) = 2.60 < x < 3.0 m
Computation number of lanes for the left corridor
Width of the left corridor w = 2.60 m
The width of the corridor is smaller than 3.10 (i.e., 2 · 0.20 + 2 · 0.60 + 1.50), so:
Number of lanes L = 1 lane
Computation number of lanes for the right corridor
Width of the right corridor w = 5.70–3.0 = 2.70 m
The width of the corridor is smaller than 3.10 (i.e., 2 · 0.20 + 2 · 0.60 + 1.50), so:
Number of lanes L = 1 lane
Maximum flow rate per corridor when disentangling both corridors
Maximum flow rate = 2 · 30.77 = 61.54 persons per minute
Flow rate threshold
Flow rate threshold T_q = min(92.31, 61.54) = 61.54 persons per minute = 1.03 persons per second

In addition, the density threshold is impacted by group dynamics in a space. Here, the allowable physical distancing density increases when groups of people are present. The density threshold T_k for a mixed crowd can be determined using Eq. (11), where P_g represent the percentage of 1- to g-person groups in the crowd (potentially at a particular moment in time t), N_g the number of individuals in a g-person group, and A_g the minimum area occupied by a g-person group. Here, depending on the crowd monitoring system, an average P_g can be determined or $P_g(t)$ can be determined in real-time, thus making the density threshold dynamic. This mathematical formulation determines the average number of individuals present for a particular distribution of group sizes and divides it by the average area required by that particular distribution of groups. The percentages of various group sizes should add up to 1.

$$\mathrm{T_k} = \frac{\sum_g P_g \cdot N_g}{\sum_g P_g \cdot A_g} \tag{11}$$

Also, in the case of grouping, this particular computation will provide a very optimistic estimation of the maximum density because the exact constellations of the groups have not been considered. The underlying assumptions of this equation are that groups will be equally distributed over space and time, space allows these groups to be distributed optimally, and the space layout allows for complete utilization of the space (i.e., no walkable area goes unused).

3.6. Interactions computation and threshold determination

The last KPI of the physical distancing capacity framework is the interactions $I(t)$, where an interaction is defined as any occurrence of a distance smaller than the local physical distancing rule between any two individuals that are not related, in which we normalize the number of interactions by the number of people present at the moment $N(t)$ (see Eqs. (12) and (13)). Here, $d_{p,q}$ represents the distance between a pedestrian of focus p and another pedestrian in its vicinity q. To monitor whether interactions occur, it is essential to monitor the distance between all individuals in the crowd. Calibrated stereovision and depth sensors can provide this information at a relatively high framerate. Here, we assume that people follow the physical distancing regulations pertaining to interactions with unrelated individuals.

$$i_{p,\mathrm{q}}(t) = \begin{cases} 0 & d_{p,q} \geq 1.50 \\ 1 & d_{p,q} < 1.50 \end{cases} \tag{12}$$

$$I(t) = \frac{1}{2}\sum_p \sum_q i_{p,q}(t) \cdot \frac{1}{N(t)} \tag{13}$$

In crowded pedestrian infrastructure, pedestrian operational movement dynamics fluctuate quickly. Therefore, infrequent snapshots of a crowd might not identify non-compliance issues. Interactions might be very short in nature, especially at the border between lanes moving in opposite directions, but can potentially temporarily encroach on the physical distancing rule. Thus, also for this measure, it is important to monitor this behavior at a relatively high frequency. To balance this KPI with the other two variables, the authors have adopted (again) a frequency of 4 frames per minute for this computation.

No interactions should be allowed when only unrelated pedestrians move through pedestrian infrastructure. As such, the threshold for a 1-person group is 0. However, some interactions between relatives should be allowed when groups are present in a crowd. Filtering the interactions allowed from the real-time data stream is often challenging to achieve, computationally intensive, and prone to error. Instead, the authors have opted for a dynamic interactions threshold T_I, which can be adapted to the percentage of groups of a specific size in the crowd P_g and the group size N_g for a given context (see Eq. (14)). Please note that individuals are accounted for in this formulation as a 1-person-group. The total interactions allowed within a group of a specific size can be determined by the (N-1)$^{\mathrm{th}}$ triangle number.

$$\mathrm{T_I} = \sum_g \frac{N_g \cdot P_g}{\sum_g N_g \cdot P_g} \cdot \frac{N_g(N_g - 1)}{2} \cdot \frac{1}{N_g} \tag{14}$$

4. Case study 1: The vondelpark

This section applies the physical distancing capacity framework to assess a busy location in Amsterdam, the Vondelpark, where public safety concerns were raised. It begins with a brief introduction to the case, followed by the results for the three KPIs. The section concludes with key insights gained from the framework's implementation at this location and recommendations for optimizing crowd management.

4.1. Introducing the Vondelpark case study

The Vondelpark is a public park located at the rim of the city center of Amsterdam. Locals and tourists alike frequently visit this park. On a typical Saturday, you will find pedestrians and cyclists jointly using the shared space paths along the park's length. The population is very diverse in age, gender, and group size.

On weekdays, the Vondelpark is most busy in the late afternoon. On weekends, the park gets incrementally busier until approximately 16:00, after which the total demand slowly declines until sundown. In the mornings, people predominantly walk and cycle

over the paths, while during (sunny) afternoons, most people in the park congregate in groups on the lawns.

This case study evaluates to what extent the capacity of a shared space path and its sidewalks near the main entrance of the Vondelpark (i.e., Stadhouderskade entrance) is exceeded during a busy period. In particular, the study showcases one hour of monitoring data between 12:00 and 13:00 on Friday, June 12th, 2020, which is the time with the highest demand during this particular day. On the day the data for this case study was captured, the weather was not bad by Dutch standards (i.e., maximum temperature 26.1C°, clouded, 11.1 mm rain in the evening, little wind – 4.5 m/s). Consequently, people were using the park as they would typically do.

The monitoring system was installed downstream of the northern main entrance of the park. Stereovision sensors were installed in two poles in the middle of the path. See Fig. 4 for a picture of the park and the layout of the monitoring area. As one can see, pedestrians and cyclists can pass the monitoring installation on three sides: the left, the middle, and the right. The trajectory data captured at this location shows that the people (i.e., a mixture of pedestrians and cyclists) slightly prefer to pass in the middle of the sensors. Moreover, because the monitoring system is located in a shared space, some cyclist trajectories have been captured by the monitoring system. The cyclists' trajectories will also be treated as pedestrians for this showcase because we cannot properly distinguish between the two modes, as there may have been pedestrians with high speeds (i.e., runners) and cyclists with low speeds.

4.2. Flow rate assessment

The flow rate threshold is determined using the computation depicted in Table 3. Here, we assume an average walking speed of 1.0 m/s. In this case, the sensor equipment is located in a relatively open shared space. However, the trees on the sidewalks usually limit the number of lanes that can be formed. Thus, instead of the 8 lanes, only 7 fit in the available walkable area. As a result, the flow rate threshold is 3.59 persons per second.

The flow rate recorded at the Vondelpark is visualized in Fig. 5.A. As one can see, the flow rate (i.e., the average flow rate per 15 s) fluctuates with time. Several peaks can be distinguished at 12:02, 12:16, 12:55, and 12:57. These sudden changes in the flow rate suggest that one is likelier to see temporally minor violations of the flow rate threshold than temporally elongated violations at this location. Yet, even at this hour, the flow rate does not reach the flow rate threshold. During the highest peak (1.13 persons per second), $S_q(t)$ is roughly 0.31 (i.e., 1.13/3.59). This means that 31% of the flow rate capacity is used at that moment. The maximum flow rate

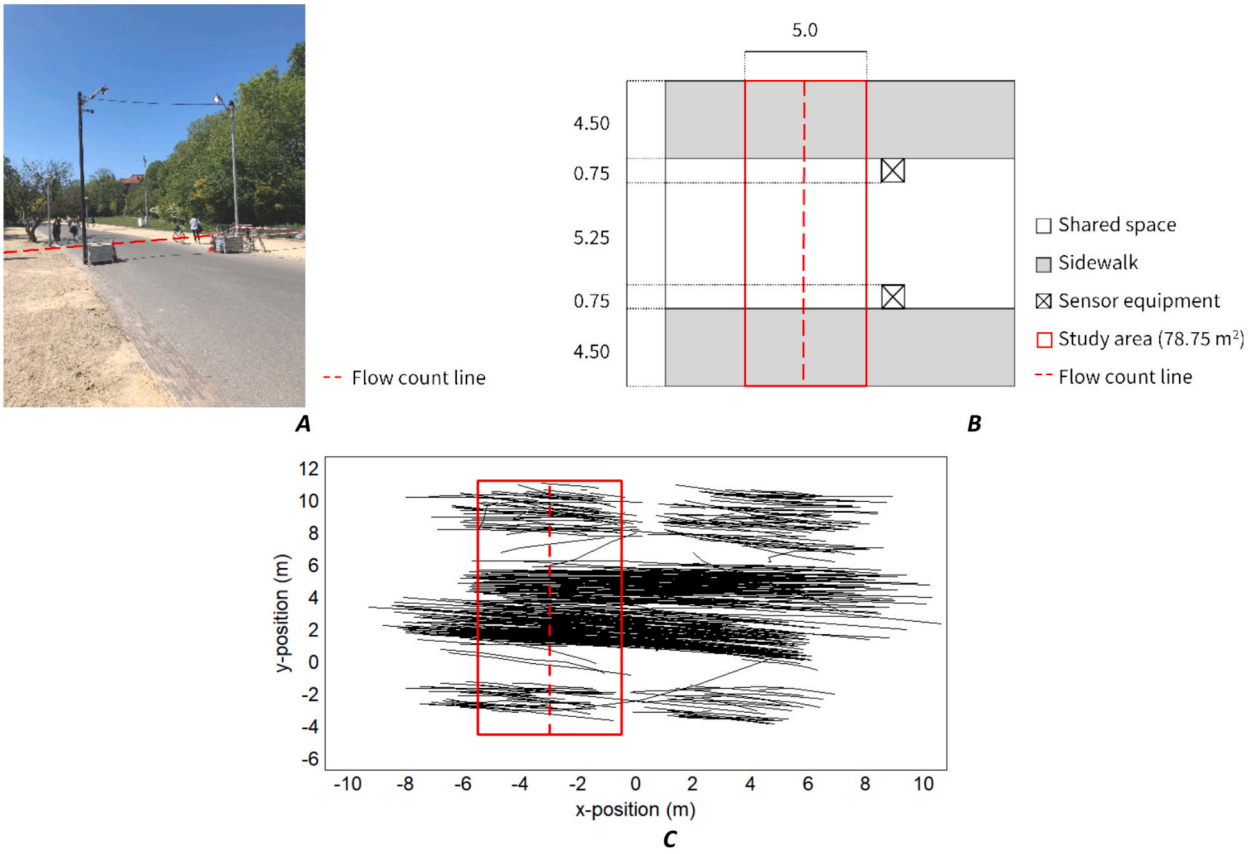

Fig. 4. Visualization of the monitoring area at the Vondelpark (A), the layout of the monitoring area (B), and the trajectories of a subset of pedestrians (C).

Table 3
Computation of the flow rate threshold T_q of the Vondelpark.

Infrastructure and population characteristics
Width of the corridor $w = 15.75$ m
Average walking speed $\bar{v} = 1.0$ m/s
Additional infrastructure characteristics for compartment 2 (i.e., shared space)
Location of the obstacle (i.e., sensing equipment) = $0.0 < y < 0.75$ m and $6.0 < y < 6.75$ m
Computation maximum flow rate per lane
Total longitudinal spacing = $1.50 + 0.45 = 1.95$ m
Time required for one person to pass the cross-section safely = $1.95 / 1.0 = 1.95$ s
Total number of pedestrians per lane that can pass in one minute $q_{lane}^{max} = 60 / 1.95 = 30.77$ persons per lane
Computation number of lanes full length (15.75 m)
The width of the corridor is larger than 3.10 m (i.e., $2 \cdot 0.20 + 2 \cdot 0.60 + 1.50$), and
The required space per extra pedestrian is 2.10 m (i.e., $0.60 + 1.50$), so:
Number of lanes $L = 2 + \text{floor}((15.75 - 3.10) / 2.10) = 8$ lanes
Computation compartments 1 and 3 (4.50 m) (i.e., sidewalks)
The width of the corridor is larger than 3.10 (i.e., $1 \cdot 0.2 + 1 \cdot 0.60 + 1.50$), and
The required space per extra pedestrian is 2.10 m (i.e., $0.60 + 1.50$), *so:*
Number of lanes $L = 2 + \text{floor}((4.50–3.10) / 2.10) = 2$ lanes (per compartment)
Computation compartment 2 (5.25 m) (i.e., shared space)
The width of the corridor is larger than 3.10 (i.e., $1 \cdot 0.2 + 1 \cdot 0.60 + 1.50$), and
The required space per extra pedestrian is 2.10 m (i.e., $0.60 + 1.50$), so:
Number of lanes $L = 2 + \text{floor}((5.25–3.10) / 2.10) = 3$ lanes
Flow rate threshold
Flow rate threshold $T_q = \min(2 + 2 + 3, 8) \cdot 30.77 = 215.39$ persons per minute = 3.59 persons per second

per 15 s exceeds the threshold multiple times, which is allowed, as 7 people (one per lane) can safely pass per second (see Table 3), provided it doesn't consistently surpass this rate. A minimum longitudinal spacing of 1.95 s must be maintained, assuming a walking speed of 1.0 m/s.

4.3. Density assessment

At the Vondelpark, individuals and pairs were registered by the authors at approximately 80% and 20% respectively. The area that one individual requires is 4.10 m^2, while for a group of two individuals walking abreast, the space requirement per person decreases to 2.93 m^2 (i.e., 5.85/2). Given the computation mentioned in Eq. (11), the density capacity of the Vondelpark case study area is 0.270P/m^2 (i.e., $\frac{0.80 \cdot 1 + 0.20 \cdot 2}{0.80 \cdot 4.10 + 0.2 \cdot 5.85}$).

Fig. 5B depicts the density development at the Vondelpark over time. This location's density (i.e., the average density per 15 s) is more stable than the flow rate. This suggests that people have the space to evade each other without issues. The highest density encountered is 0.031P/m^2 (at 12:02), which results in an $S_k(t)$ of 0.11 (i.e., 0.031/0.270). This means that approximately 11% of the density capacity is used at that moment. Also, the maximum density per 15 s are well below the density threshold.

4.4. Interactions assessment

Only groups of two or more individuals are allowed to interact, where the exact number of allowed interactions depends on the group's size. The estimated percentages of singles and pairs in the Vondelpark case study suggest that for every ten groups, two interactions are allowed (i.e., $10 \cdot [0.80 \cdot 0 + 0.20 \cdot 1] = 2$).

Using Eq. (14), the interactions capacity of the Vondelpark case study area is 0.167 (normalized) interactions (i.e., $\frac{0.80 \cdot 1}{0.80 \cdot 1 + 0.20 \cdot 2} \cdot \frac{1 \cdot (1-1)}{2} \cdot \frac{1}{1} + \frac{0.20 \cdot 2}{0.80 \cdot 1 + 0.20 \cdot 2} \cdot \frac{2 \cdot (2-1)}{2} \cdot \frac{1}{2}$). Fig. 5C illustrates that the number of interactions (i.e., the average interactions per 15 s) frequently encroach on the interactions threshold. That is, $S_I(t)$ is often 1. Consequently, this measurement suggests that the safe capacity in the Vondelpark is already met.

4.5. How to interpret and act on the Vondelpark measurements

As a result of the high $S_I(t)$, $S_{KPI}(t)$ is often 1. This suggests that the physical distancing capacity of this location is exceeded, and crowd management actions are required. The flow rate and density measurements provide no reason for concern, given that both

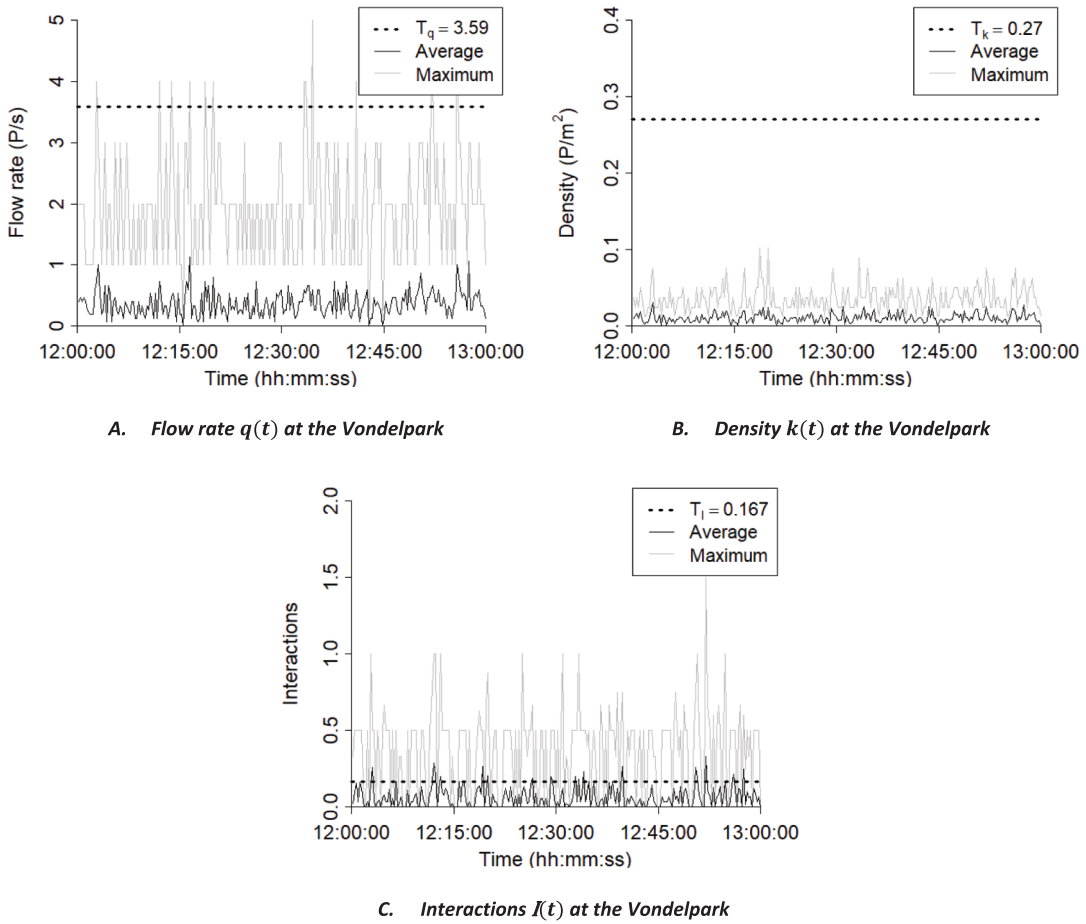

A. Flow rate $q(t)$ at the Vondelpark

B. Density $k(t)$ at the Vondelpark

C. Interactions $I(t)$ at the Vondelpark

Fig. 5. Monitoring data for the Vondelpark case study, with average and maximum KPI values per 15 s, and the KPI thresholds represented by a dashed line.

measurements are generally well within the maximum limits. The relatively high number of interactions at some moments in time does, however, suggest that people either find it difficult to adhere to the physical distancing regulations or they walk in 2- to g-person groups in which interactions are allowed (i.e., households). In case of compliance issues with the physical distancing regulations in the Vondelpark case, crowd management measures should be aimed at optimizing the distribution of individuals and groups over the available infrastructure. Examples of this type of crowd management measures are variable message signs with alerting messages, visuals that make the physical distancing regulations explicit, and hosts that alert people when the physical distancing regulations are not adhered to properly.

5. Case study 2: Utrecht central station

This section presents a second case study, conducted at Utrecht Central Station, one of the largest transfer hubs in the Netherlands. Unlike the Vondelpark, this location is more consistently crowded and differs significantly in terms of population and pedestrian movement dynamics. The section begins with a brief introduction to the case, followed by the results for the three KPIs. It concludes with key insights from the framework's implementation at this location and recommendations for improving crowd management.

5.1. Introducing the Utrecht Central station case study

The second case study features a section of the walkable space inside Utrecht Central station. This space features an intersection area along one of the main routes through the transfer station. Train travelers ascend the stairs at the top of Fig. 6B to enter the station's main hall or descend towards train platforms 5 and 7. The escalator at the bottom of Fig. 6B points in the other direction. As such, travelers will not enter the depicted intersection area from the escalator. Next to the movements through the station and to and from the platforms, travelers can also visit one of the two shops on the top right and left of Fig. 6B.

These movements jointly result in the trajectory dataset visualized in Fig. 6C. As one can see, the dominant movements are left–right and right-left, which naturally split into two lanes. Most individuals crossing the main flow originate from within or join the

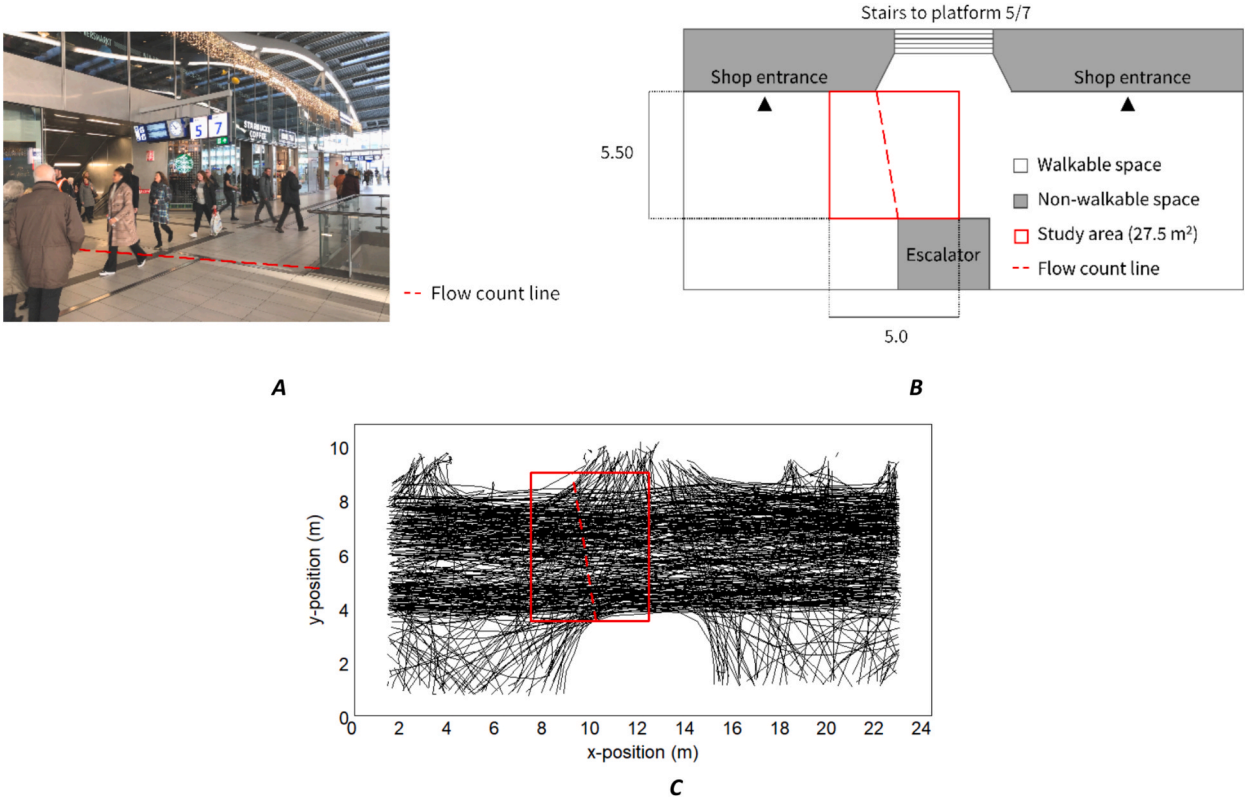

Fig. 6. Visualization of the monitoring area at Utrecht Central station (A), the layout of the monitoring area (B), and the trajectories of a subset of pedestrians (C).

main flow. Infrequently, travelers attempt to cross the main flow from the lower left and lower right to the top left or right.

During the COVID-19 pandemic, most people were asked to work from home. Consequently, contrary to what one would expect, this particular station is currently most busy on weekend days. The Utrecht Central station case study features the busiest hour of Saturday, June 20th, 2020, namely from 12:00 to 13:00. During this hour, the monitoring system identified 2129 individuals. Only 1125 of those individuals passed the flow count line in the study area as depicted in Fig. 6.

5.2. Flow rate assessment

The flow rate threshold is determined through the computation depicted in Table 4. Again, we assume an average walking speed of 1.0 m/s. In this particular case, the capacity of the main flow is determined (i.e., the departing and/or arriving main flow). The

Table 4
Computation of the flow rate threshold T_q of Utrecht Central station.

Infrastructure and population characteristics
Width of the corridor $w = 5.50$ m
Average walking speed $\bar{v} = 1.0$ m/s
Computation maximum flow rate per lane
Total longitudinal spacing = 1.50 + 0.45 = 1.95 m
Time required for one person to pass the cross-section safely = 1.95 / 1.0 = 1.95 s
Total number of pedestrians per lane that can pass in one minute q_{lane}^{max} = 60 / 1.95 = 30.77 persons per lane
Computation number of lanes full length (5.50 m)
The width of the corridor is larger than 3.10 m (i.e., 2 · 0.20 + 2 · 0.60 + 1.50), and
The required space per extra pedestrian is 2.10 m (i.e., 0.60 + 1.50), so:
Number of lanes L = 2 + floor((5.50 – 3.10) / 2.10) = 3 lanes
Flow rate threshold
Flow rate threshold $T_q = 3 \cdot 30.77 = 92.31$ persons per minute = 1.54 persons per second

intersecting movements are not explicitly accounted for in the flow rate threshold computation. Using the physical distancing capacity framework, we find that 3 lanes fit in the walkable area, which results in a flow rate threshold of 1.54 persons per second.

The flow rate recorded at Utrecht Central station is visualized in Fig. 7A. As one can see, the flow rate (i.e., the average flow rate per 15 s) fluctuates rapidly over time. Two prominent peaks can be distinguished at 12:06 and 12:50. The flow rate does not reach the flow rate threshold. During the highest peak (1.27 persons per second), $S_q(t)$ is 0.82 (i.e., 1.27/1.54), meaning 82% of the flow rate capacity is used. In this case, the maximum flow rate per 15 s also exceeds the threshold multiple times, which is allowed as long as it doesn't consistently do so. However, only 3 people (one per lane) can safely pass per second (see Table 4), while instances of 4P/s have been observed, indicating that people could not keep a safe distance. Additionally, the frequent proximity of the maximum flow rate to the number of lanes indicates that the minimum longitudinal spacing of 1.95 s (assuming a walking speed of 1.0 m/s) may not be maintained.

5.3. Density assessment

At the train station, the percentage of groups is lower than in the Vondelpark. Based on the authors' observations, most groups feature one (90.5%) or two (9.5%) individuals. Using the group percentages and the spatial requirements of the various group sizes, the density threshold for this particular area of the train station is 0.257P/m^2 (i.e., $\frac{0.905 \cdot 1 + 0.095 \cdot 2}{0.905 \cdot 4.10 + 0.095 \cdot 5.85}$).

Fig. 6B illustrates the density in the monitored area. The density (i.e., the average density per 15 s) is generally relatively low, with sharp increases around the moments when the flow rate was also found to peak. The highest measured density within the study period is 0.184P/m^2, which results in a $S_k(t)$ of 0.72 (i.e., 0.184/0.257). This means that 72% of the density capacity is used within this region's 'safe' density limits. At the same time, the maximum density per 15 s is well above the density threshold of 0.257P/m^2. This can be a local fluctuation, but it provides cause for concern and signals that too many people reside in the same infrastructure at some point in time.

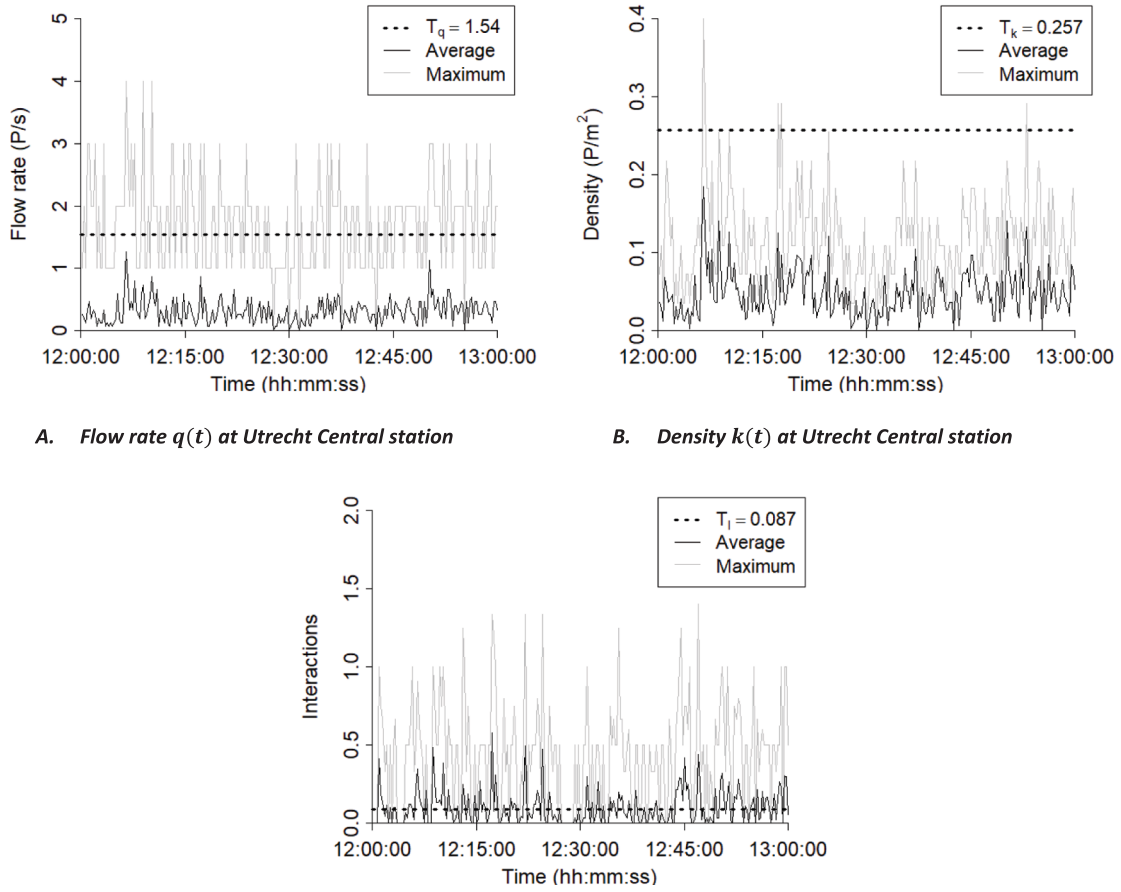

A. Flow rate $q(t)$ at Utrecht Central station

B. Density $k(t)$ at Utrecht Central station

C. Interactions $I(t)$ at Utrecht Central station

Fig. 7. Monitoring data featuring the Utrecht Central station case study, with average and maximum KPI values per 15 s, and the KPI thresholds represented by a dashed line.

5.4. Interactions assessment

The last KPI for the Utrecht Central station case is determined similarly as was adopted for the Vondelpark case study. Using the percentages for the different group sizes, the interactions capacity of the Utrecht Central station case study is 0.087 (normalized) interactions (i.e., $\frac{0.905 \cdot 1}{0.905 \cdot 1 + 0.095 \cdot 2} \cdot \frac{1 \cdot (1-1)}{2} \cdot \frac{1}{1} + \frac{0.095 \cdot 2}{0.905 \cdot 1 + 0.095 \cdot 2} \cdot \frac{2 \cdot (2-1)}{2} \cdot \frac{1}{2}$). Fig. 7C illustrates that the interactions threshold is frequently exceeded. Consequently, also, in this case, the pedestrian infrastructure has exceeded its 'safe' interactions capacity.

5.5. How to interpret and act on the Utrecht Central station measurements

This case study has shown that during a relatively busy Saturday in June 2020, the flow rate and density both remained within their capacity limits. However, the interactions capacity was exceeded frequently during the hour of focus. In contrast to the Vondelpark case, the flow rate and density measurements are already a lot closer to the capacity thresholds. Consequently, crowd management strategies that solely focus on improving the interaction behavior of the crowd will most likely not be sufficient to improve the situation. Instead, crowd management measures are advised that aim at reducing the flow rate and density at this specific location in Utrecht Central station. Example of this type of crowd management measures are the local rerouting of travellers by means of variable message signs and the creation of one-directional flow scenario in which overtaking is prohibited.

6. Lessons learned from applying the physical distancing capacity framework

The previous two sections applied the physical distancing capacity framework to two very different cases during the COVID-19 pandemic: a park - the Vondelpark - and a large transfer hub - Utrecht Central station. The implementation provides three important insights regarding the functioning of the physical distancing capacity framework.

First and foremost, this capacity framework uses three distinct KPIs: flow rate, density, and interactions. Theoretically, the thresholds of both the flow rate and the interactions KPI can be exceeded independently of the other two. The two case studies show that the three KPIs indeed fluctuate independently. Consequently, to ensure all potential breaches of the physical distancing regulations are detected, it is important to retain all three KPIs within the physical distancing capacity framework.

Yet, the case studies illustrate that the interactions KPI is often the first to exceed the capacity threshold. A more in-depth analysis of the relationship between the density and the interactions (see Fig. 8) provides clear indications pertaining to why this occurs. An approximately linear relation is found between the density and the interactions. Unsurprisingly, it becomes more difficult to keep one's distance when density increases. However, counter-intuitively, at very low densities, a relatively high number of interactions was identified in both case studies. Moreover, a highly fluctuating number of interactions is found at one density level. These two findings imply that also, at low density levels, pedestrians find it difficult to adhere to the physical distancing regulations. Consequently, people's behavior has a potentially larger impact on the safety of pedestrian infrastructure than the actual size and layout of the available walkable area.

One could be inclined to use one KPI instead of three, given that the interactions KPI is most likely the first to violate the capacity. The authors advise against this line of reasoning because the two case studies also show that combining the three KPIs provides more specific directions for crowd management action. For example, when the number of interactions is exceeded, but the flow rate and density are relatively low, crowd management measures to change behaviour can be very effective. At the same time, when the flow rate and/or density KPI encroach their thresholds, this type of measures is of little use. Similarly, when the density is at capacity, but

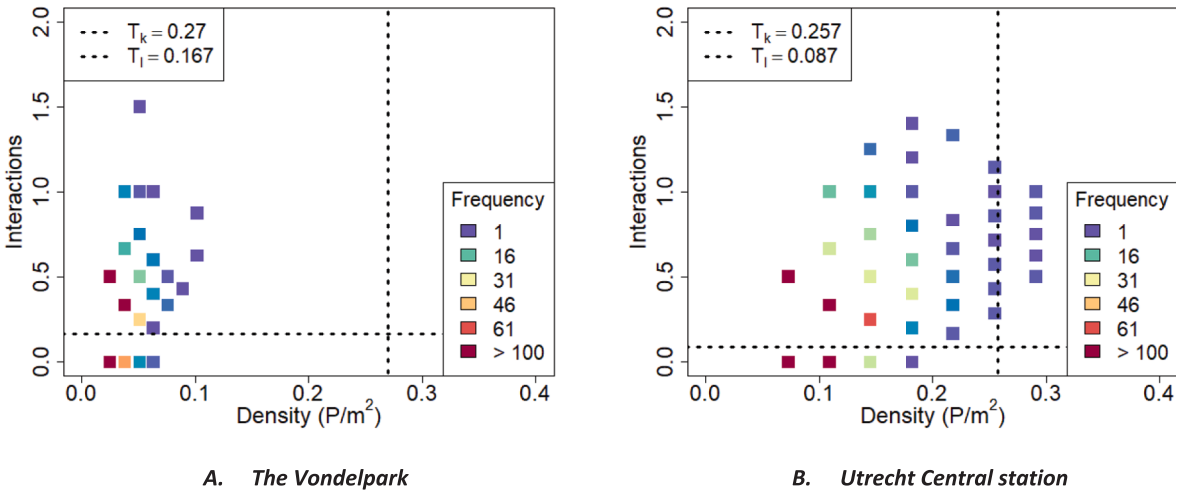

Fig. 8. Relationship between density and interactions per screen capture (i.e., one per second) for the Vondelpark (A) and Utrecht Central station (B), with dashed lines indicating the respective density and interactions thresholds. Only measurements involving at least two people are shown.

the flow rate is relatively low, crowd management measures aimed at increasing the flow rate (e.g., waving people along to keep people from standing still and limiting the size of waiting areas) can improve the situation. When the flow rate is also high, restricting access to the area is potentially more effective. The combination of the three KPIs provides clear indications regarding the most effective course of action to resolve potentially unsafe situations.

7. Applying the physical distancing capacity framework to pedestrian infrastructure design and management

Luckily, anno 2024, COVID-19 is not rampaging through the world anymore. Does this mean that the physical distancing capacity framework has lost its relevance? Our answer to that question is no for two reasons. Firstly, COVID-19 is unfortunately not the first or last airborne disease that will disrupt public life in the future. Thus, even though not relevant for 'normal' day-to-day crowd management, it is essential to keep it lying on the shelf for the moment when we encounter a new airborne disease with similar properties. Secondly, the physical distancing capacity framework provides clear pointers regarding the resilient design of pedestrian infrastructure. During the first months of the COVID-19 pandemic, life partly came to a standstill because most pedestrian infrastructure could not be safely used without a high risk on mass spreading events. Underneath, the framework's application for (real-time) crowd management purposes and resilient pedestrian infrastructure design are further elaborated on.

7.1. Real-time crowd management using the physical distancing capacity framework

The physical distancing capacity framework is developed for real-time crowd management. In particular, the KPIs in the framework provide insights to crowd management organizations regarding which interventions are useful for which scenario. Table 5 depicts the most relevant KPI combinations. One or more KPIs will infringe on its threshold depending on the circumstances. For each KPI, distinct crowd management measures are more or less effective. For instance, when the flow rate KPI is high, inflow limitation will be sufficient to limit the pressure within pedestrian infrastructure, while behavioral measures will resort to limited effect. When the density KPI is high, there are simply too many people in too-small infrastructure. Asking people to leave is then the only available solution. When only the interactions KPI is too high, one or more individuals stand too close together. This would ask for any behavioral measure that disperses the crowd while allowing everyone to remain in the same infrastructure. Similarly, for all KPI com, one can determine whether interventions are necessary for all KPI combinations one can determine whether interventions are required. When interventions are necessary, the framework will also provide guidance regarding which interventions will have the most effect.

Table 5 also identifies that the interaction KPI is most likely to infringe on its threshold first. So, why should one not only monitor the interactions KPI? This is because the required crowd management actions partly depend on the other two KPIs (i.e., the flow and density state). When the density KPI is low, dispersing the crowd is sufficient. However, when the density KPI is also high, dispersing the crowd will not have enough effect and can potentially lead to annoyance in the crowd and risky transmission scenarios. In the latter case, additional measures need to be taken to ensure the crowd's density does not increase further; for instance, by actively asking people to move towards another area.

The conditions in pedestrian infrastructure vary continuously and can quickly deteriorate. Therefore, one should remember that for real-time crowd management, one also requires a crowd management organization that can intervene rapidly when the KPIs encroach on the thresholds at a moment's notice. To ensure rapid interventions, a real-time crowd management organization for health purposes requires:

- Real-time monitoring systems in relevant locations,
- Real-time data communication, filtering, and KPI assessment,
- Real-time action selection mechanism, and
- Set of human or digital actuators to intervene when necessary.

It is important to note that the activation of interventions takes time. One should account for a response time of 5 to 30 min, depending on the severity of the measures. Therefore, any monitoring system and set of KPI thresholds should leave room for the situation to deteriorate while one is activating the interventions. Moreover, the very rapidly changing conditions also require a crowd monitoring system that frequently evaluates the current state of the infrastructure (e.g., at least one evaluation per minute). Otherwise, rapid fluctuations within the infrastructure will be missed (e.g., a large crowd exiting a train that just arrived).

Besides the control system parts, one should also have prepared the exact threshold values for the specific context. Next to a quantitative description of the condition'unacceptable', it is also advised to pre-emptively discuss with all stakeholders which KPI

Table 5
Crowd management actions for relevant KPI combinations.

Flow rate	Density	Interactions	Crowd management action
Low	Low	High	Take behavioural measures to disperse the crowd
Medium	Medium	Low	Do nothing, crowd attempts to do the right thing
Medium	High	High	Disperse the stationary crowds, and limit inflow
High	Medium	High	Limit the inflow, increase outflow
High	High	High	Limit the inflow, increase outflow, and disperse the crowd

values triggers which crowd management measures. We have experienced that thoroughly embedding the framework into the organization and its procedures creates efficiency and effectiveness at the moments that count.

7.2. Designing resilient pedestrian infrastructure

In addition to using the physical distancing capacity framework for real-time crowd management purposes, it can also be used to design pedestrian infrastructure and evaluate its functioning pre-emptively or after the fact. Here, pedestrian infrastructure design entails more than a layout; it also includes the origin-destination matrix, activity scheduling patterns, and demand profile of a venue. In contrast to real-time monitoring to resolve potentially dangerous transmission cases quickly, pre-emptive and after-the-fact evaluations aim to improve the pandemic preparedness of pedestrian infrastructure in the longer run (weeks, months, or years).

The focus of the analysis changes in the case of resilient pedestrian infrastructure design. It becomes: 'Under which conditions can pedestrian infrastructure keep functioning during a pandemic resulting from a dangerous airborne human-to-human transmittable virus?' The same three KPIs can be applied in combination in a backward manner. That is, one reasons from the acceptable safety levels to the KPI threshold values, and accordingly from the KPI threshold values to the acceptable demand profile, activity patterns, and crowd dynamics in the venue. Accordingly, one can compare one's expectations regarding the crowd dynamics with those that can be safely sustained in pedestrian infrastructure. In complex cases, crowd simulation programs can further substantiate one's expectations regarding crowd dynamics.

When operationalizing the KPI thresholds in acceptable demand profiles, activity patterns, and crowd dynamics, the three KPIs will automatically tackle various properties of the pedestrian infrastructure design. Table 6 displays the additional design requirements the KPI framework poses to prepare pedestrian infrastructure for a pandemic. We expect that when one applies these additional design requirements, the dimensions of prepared public venues will increase. In some cases, these larger dimensions are not realistic. In those cases, one will need to use crowd management (see section 7.1) to limit the flow, densities, and interactions within the venue.

Please note, in both case studies, the interactions KPI was the one that encroached on the safety threshold values first. This suggests that pedestrians find it very difficult to adhere to physical distancing regulations, even when sufficient space is available. Consequently, pedestrian infrastructure design that caters for pandemic preparedness ensures that a) there is sufficient space available for essential traffic that needs to make use of the pedestrian infrastructure during a pandemic using the design requirements in Table 6 and b) ensures that the individuals that make use of the pedestrian infrastructure are empowered to follow the regulations. The latter includes but is not limited to a) gentle reminders of the governing regulations and the impact of their choices on the safety of surrounding individuals, b) a spatial design that naturally supports the separation of flows within the venue and prevents choke points and c) an activity schedule that supports the distribution of pedestrian demand over time and space.

8. Conclusions and future work

This paper presented a new capacity framework for designing and managing pedestrian infrastructure under physical distancing regulations. This framework determines the 'safe' capacity utilizing three key performance indicators (KPIs): flow rate, density, and interactions. The framework incorporates a parameterization of the physical distancing regulations of the various countries and the latest knowledge on pedestrian operational movement dynamics. Two years after the COVID-19 pandemic, this paper contributes to the literature by reflecting on the lessons learned regarding the development and implementation of a (physical distancing) capacity framework that can aid the design and management of crowded pedestrian infrastructures.

Using two case studies, this paper shows that the physical distancing capacity framework provides clear indications regarding when and why pedestrian infrastructures become unsafe. Furthermore, they illustrate that two metrics, i.e., the flow rate and interactions KPI, can independently encroach on their capacity thresholds. Where the flow rate KPI quantifies to what extent potentially more throughput can be safely handled, the interactions KPI quantifies the extent of the crowd's (unintentional) non-compliance behavior. The third KPI (i.e., the density KPI) cannot independently infringe on the safety thresholds but is essential to better understand the potential of various management strategies. A combination of all three metrics (i.e., including the density KPI) provides more specific guidance regarding follow-up crowd management actions to ensure the safety of pedestrian infrastructure during respiratory virus pandemics, such as the COVID-19 pandemic.

The study also revealed two potential areas of improvement in the physical distancing capacity framework. Firstly, the current framework makes assumptions on the most likely spatial constellation of groups and the even distribution of groups over space and time. A validation study is required to establish whether these assumptions are valid in practice. Secondly, the three metrics featured in the physical distancing capacity framework can heavily fluctuate over time and space, requiring careful interpretation of the metrics when choosing follow-up crowd management actions. Hence, a thorough embedding of the framework in crowd management organizations is essential to fully leverage the potential of the framework. Extensive legwork is required within governing bodies and crowd management organizations to ensure the correct embedding of the (physical distancing) capacity framework.

Besides these two potential improvements, two essential steps in further operationalizing the capacity framework are identified. Firstly, it is imperative that this new framework is validated. Here, in particular, validation of the underlying assumptions and the normative scenarios is sought after in close collaboration with operational crowd managers. Besides that, this framework is now only useful when it is adopted by practice as a tool to improve the crowd management of pedestrian infrastructure during respiratory virus pandemics. The backbone of the physical distancing capacity framework can, however, also be extended to aid the design and crowd management of crowded spaces under non-pandemic conditions, for example, to improve other safety aspects (e.g., physical or social safety). An open dialogue with crowd management professionals is required to establish which metrics best describe these safety

Table 6
Design requirements for pandemic preparedness of pedestrian infrastructure.

KPI	Design requirements
Flow rate	A) Incorporate wider cross-sections in the design to allow for a lower flow capacity under physical distancing regulations
Density	B) Incorporate additional storage capacity in the design to allow for a lower maximum density under physical distancing regulations
Interactions	C) Incorporate wider interaction spaces (intersecting points, overtaking, etc.) in the design to allow for the additional required space to interact safely under physical distancing regulations.D) Separate pedestrian flows, as much as possible, by design utilizing the scheduling of activities and planning of activity locations.

aspects under different crowd conditions.

CRediT authorship contribution statement

Lucia van Schaik: Conceptualization, Methodology, Software, Visualization, Formal analysis, Writing – original draft, Writing – review & editing. **Dorine Duives:** Methodology, Writing – original draft, Conceptualization, Visualization, Writing – review & editing, Funding acquisition. **Serge Hoogendoorn:** Funding acquisition, Writing – review & editing.

Declaration of competing interest

The authors declare that they have no known competing financial interests or personal relationships that could have appeared to influence the work reported in this paper.

Acknowledgements

This research was supported by the Proof of Concept project named "Intelligent Multi-modal Transfer Flow Management system (iMTFM)" - no. 899891, which is financed by the European Research Council, and the EIT KIC project "CityFlows" – no. A20003. We thank NS Stations and the Municipality of Amsterdam for allowing us to study the data from their crowd monitoring systems.

References

Banerjee, A., Maurya, A.K., Lammel, G., 2018. A review of pedestrian flow characteristics and level of service over different pedestrian facilities. Collective Dynamics 3 (A17), 1–52.
BBC.com (2020) Coronavirus: what are social distancing and self-isolation rules? Last reviewed: 31 July 2020, visited: 11 august 2020. https://www.bbc.com/news/uk-51506729.
Bian, Y., Wang, W., Lu, J., Ma, J., Tan, D., 2007. Pedestrian level of service for sidewalks in China. In: Proceedings of the 86Th Annual Meeting of the Transportation Research Board (TRB), pp. 07–1185.
Bundesregierung.de (2020). Coronavirus in Deutschland. Last edited: ?. last visited: 11 august 2020. https://www.bundesregierung.de/breg-de/themen/coronavirus/corona-massnahmen-1734724.
Cao, S., Seyfried, A., Zhang, J., Holl, S., Song, W., 2017. Fundamental diagrams for multidirectional pedestrian flows. Journal of Statistical Mechanics 2017, 033404.
Chang, Hai-Chau; Wang, Lih-Chung (2010). "A Simple Proof of Thue's Theorem on Circle Packing". arXiv:1009.4322 [math.MG].
Chattaraja, U., Seyfried, A., Chakroborty, P., 2009. Comparison of pedestrian fundamental diagrams across cultures. Adv. Complex Syst. 12 (3), 292–405.
Centers for Disease Control and Prevention (2020). What is social distancing? Last reviewed: May 6, 2020, visited: June 20, 2020. https://www.cdc.gov/coronavirus/2019-ncov/prevent-getting-sick/social-distancing.html.
Daamen, W., Hoogendoorn, S., 2010. Emergency door capacity: influence of door width, population, composition and stress level. Fire Technol. 48 (1), 55–71.
Comparing Three Types of Real-Time Data Collection Techniques: Counting Cameras, Wi-Fi Sensors and GPS Trackers PED2016, 2016, 568–574.
Dowling, R., Reinke, D., Flannery, A., Ryus, P., Vandehey, M., Petritsch, T., Landis, B., Rouphail, N. Bonneson, J. (2008). Multimodal Level of Service Analysis for Urban streets. NCHRP report, no. 616. Transportation Research Board.
Duives, D., van Schaik, L., Thiellier, E., van Dijk, J., Drewes, R., 2020. Crowdmanagement in een anderhalvemetersamenleving. NM Magazine no. 2. https://www.nm-magazine.nl/artikelen/crowdmanagement-in-een-anderhalvemetersamenleving/.
Finch, E., 2010. Pedestrian comfort level guidance. Transport for London.
Fruin, J., 1971a. Designing for pedestrians: a level-of-service concept. Highw. Res. Rec. 355, 1–15.
Fruin, J. (1971b). Pedestrian Planning and Design. New York.
Garcimartin, A., Zuriguel, I., Pastor, J., Martin-Gomez, C., Parisi, D. (2014). Experimental evidence of the "Faster Is Slower" effect. Proceedings of The Conference on Pedestrian and Evacuation Dynamics 2014 (PED2014). Transportation Research Procedia, vol. 2, pp. 760-767.
Gouvernement.fr (2020). Coronavirus COVID-19. Last updated: 22 June 2020, last visited: 11 august 2020. https://www.gouvernement.fr/en/coronavirus-covid-19.
Van Gelder, A. (2018). Drukte op het perron en de impact op reizigersbeleving, NS Stations.
Gorrini, A., Vizzari, G., Bandini, S. (2015). Granulometric distribution and crowds of groups: focusing on Dyads. Proceedings of Traffic and Granular Flow '15, pp. 273 - 280. Springer.
Greenshields, B. D., Bibbins, J. R., Channing, W. S., & Miller, H. H. (1935, December). A study of traffic capacity. In Highway research board proceedings (Vol. 14, No. 1, pp. 448-477).
Grolle, J., 2016. Perception of crowdedness, safety and atmosphere in large groups of people. Delft University of Technology. BSc. thesis.
Haghani, M., Sarvi, M., Shahhoseini, Z., 2020. Evacuation behaviour of crowds under high and low levels of urgency: experiments of reaction time, exit choice and exit-choice adaptation. Saf. Sci. 126, 104679.
Hoskam, S., 2017. The experience of safety of cyclists and pedestrians in a shared space. Delft University of Technology. BSc. thesis.
Kretz, T., Grunebohm, A., Kaufman, M., Mazur, F., Schreckenberg, M., 2006. Experimental study of pedestrian counterflow in a corridor. Journal of Statistical Mechanics. 10, P10001–P10019.
Landis, B., Vattikuti, V., Ottenberg, R., McLeod, D., Guttenplan, M., 2001. Modeling the roadside walking environment: pedestrian level of service. Transp. Res. Rec. 1773, 82–88.
Moussaïd, M., Perozo, N., Garnier, S., Helbing, D., Theraulaz, G., 2010. The walking behaviour of pedestrian social groups and its impact on crowd dynamics. PLoS One 5 (4), e10047.

Raad, N., Burke, M., 2017. Pedestrian Level-of-Service tools: problems of conception, measurement and usefulness. 39th Australasia Transport Research Forum (ATRF) 01700836.
Rijksinstituut voor Volksgezondheid en Milieu (2020). COVID-19 (nieuwe coronavirus). Last updated: ?, last visited: 11 august 2020. https://www.rivm.nl/coronavirus-covid-19.
Seyfried, A., Steffen, B., Klingsch, W., Lippert, T., Boltes, M., 2007. The Fundamental Diagram of Pedestrian Movement Revisited — Empirical Results and Modelling. In: Schadschneider, A., Pöschel, T., Kühne, R., Schreckenberg, M., Wolf, D.E. (Eds.), Traffic and Granular Flow'05. Springer, Berlin, Heidelberg.
Spain.info (2020). Practical information for tourists in the COVID-19 situation. Last updated: 10 august 2020, visited: 11 august 2020. https://www.spain.info/en/discover-spain/practical-information-tourists-covid-19-travel-spain/.
Subaih R., Maree M., Chraibi M., Awad S., Zanoon, T. (2019). Gender-based Insights into the Fundamental Diagram of Pedestrian Dynamics. In: Nguyen N., Chbeir R., Exposito E., Aniorté P., Trawiński B. (eds) Computational Collective Intelligence. ICCCI 2019. Lecture Notes in Computer Science, vol 11683. Springer, Cham.
Zanlungo, F., Brscic, D., Kanda, T., 2014. Pedestrian group behaviour analysis under different density conditions. Transp. Res. Procedia 2, 149–158.
Zanlungo, F., Brscic, D., Kanda, T., 2015. Spatial-size scaling of pedestrian groups under growing density conditions. Phys. Rev. E 91, 062810.
Zhang, J., Klingsch, W., Schadschneider, A., Seyfried, A., 2011. Transitions in pedestrian fundamental diagram of straight corridors and T-junctions. Journal of Statistical Mechanics 6.
World Health Organization (2020). Protecting yourself and others from the spread COVID-19, visited: June 20, 2020, https://www.who.int/emergencies/diseases/novel-coronavirus-2019/advice-for-public.
Reuters (2024). WHO declares end to COVID global health emergency. Last visited: September 18, 2024. https://www.reuters.com/business/healthcare-pharmaceuticals/covid-is-no-longer-global-health-emergency-who-2023-05-05/.
World Health Organization (2024). Coronavirus disease (COVID-19). Last visited: September 18, 2024. https://www.who.int/news-room/fact-sheets/detail/coronavirus-disease-(covid-19).
Atamer Balkan, B., Chang, Y., Sparnaaij, M., Wouda, B., Boschma, D., Liu, Y., Ten Bosch, Q.A., 2024. The multi-dimensional challenges of controlling respiratory virus transmission in indoor spaces: Insights from the linkage of a microscopic pedestrian simulation and SARS-CoV-2 transmission model. PLoS Comput. Biol. 20 (3), e1011956.
Rijksinstituut voor Volksgezondheid en Milieu. (2024). *Tijdlijn van coronamaatregelen 2020-2023*. Last visited: October 7, 2024. https://www.rivm.nl/gedragsonderzoek/tijdlijn-van-coronamaatregelen-2020.